Effectiveness of FDTD in Predicting SAR Distributions from the Lucite Cone Applicator

T. Samaras, *Associate Member, IEEE,* P. J. M. Rietveld, and G. C. van Rhoon, *Member, IEEE*

***Abstract*—The benefits of using superficial hyperthermia together with radiotherapy has long been proven for recurrent breast carcinomas. The lucite cone applicator has been introduced by some hospital hyperthermia units for superficial treatments. It is characterized by a large effective field size. The modeling techniques used in the past for the study of this, as well as other applicators used for superficial hyperthermia, have failed to address some treatment parameters, such as the dimensions of the waterbolus, which are significant for clinical practice. In this paper, the finite-difference time-domain (FDTD) method is used for modeling the applicators. The numerical results are compared with thermographic measurements. The agreement between predicted and measured specific-absorption-rate distributions is very good. The use of the FDTD method is expected to promote the study of treatment specific factors and help improve future treatment quality.**

***Index Terms*—Cancer, dielectric loaded waveguides, electromagnetic heating, FDTD, hyperthermia, medical treatment.**

I. Introduction

THE International Collaborative Hyperthermia Group has clearly demonstrated the benefits of combining radiotherapy with hyperthermia against radiotherapy alone in the treatment of superficial breast cancer [1]. Since the publication of the results of [1], superficial hyperthermia has become a standard treatment modality in several institutes, especially for the treatment of chest wall recurrences of breast cancer. Although it was found that clinical outcome is related to thermal dose [2], it still remains unclear which of the physical parameters of the treatment can improve its quality and, therefore, its efficacy.

The main requirements that are put forward in the development of new systems for superficial hyperthermia are the achievement of a large effective field size (EFS),[1] sufficient penetration depth[2] and good spatial control. It is usually necessary to employ an array of applicators to fulfill the above requirements.

Manuscript received November 11, 1999; revised May 3, 2000. This work was supported by the European Commission under the Training and Mobility of Researchers Grant ERB4001GT975062.

T. Samaras is with the Radio Communications Laboratory, Department of Physics, Aristotle University of Thessaloniki, GR-54006 Thessaloniki, Greece.

P. J. M. Rietveld and G. C. van Rhoon are with the Subdivision of Hyperthermia, Department of Radiation Oncology, University Hospital Rotterdam-Daniel, 3008 AE Rotterdam, The Netherlands.

Publisher Item Identifier S 0018-9480(00)09697-6.

[1]The EFS is defined as the area that is enclosed within the 50% ISO–specific absorption rate (SAR) curve at 1-cm depth inside the flat homogeneous phantom [3].

[2]The penetration depth is defined as the depth in the phantom at which the SAR becomes $1/e^2$ of its value at the surface of the phantom.

The lucite cone applicator (LCA) is a superficial hyperthermia applicator, which offers a large EFS and can be used in an array configuration. Its efficiency has been confirmed both in technical [4] and clinical [5] terms. The theoretical modeling of the applicator with the Gaussian beam model (GBM) has given very good agreement with the experimental results for some general configurations [6], [7]. However, for the modeling of more clinical realistic configurations, the GBM has a number of limitations. The GBM cannot take into account the finite size of the waterbolus, which is placed between the applicator and patient in order to couple the electromagnetic energy into the body and to control the skin temperature. Another disadvantage of the GBM is that it cannot predict correctly the coupling between the applicators in an array [6], [7]. These problems of the GBM can be overcome if electric-field measurements are performed before modeling for every treatment configuration, but this is a cumbersome task. Finally, the GBM cannot deal with tissue inhomogeneities or oblique applicator positions that are present in the clinical situation.

In this paper, it will be shown that it is feasible to theoretically study both the LCA and older applicators used for superficial hyperthermia with the finite-difference time-domain (FDTD) technique. This numerical method allows the use of a more realistic model, but is more expensive in computational resources compared to the GBM. The major advantage of the FDTD method is that it allows a three-dimensional (3-D) analysis of the applicator configurations, without the need for time-consuming measurements. Quantities like the penetration depth and EFS can directly be deduced from the calculated results. Using this sort of 3-D analysis, in the future, we expect to gain an insight in the significant parameters of the treatment leading to treatments of better quality.

II. Materials and Methods

A. LCA

The conventional applicator (CA) that has been used in the past for superficial hyperthermia consists of a water-filled rectangular waveguide that ends to a horn antenna. The waveguide is made of brass and operates at TE_{10} mode at 433 MHz. The waveguide dimensions are 3 cm $\times$ 5 cm and the aperture size of the radiating antenna is 10 cm $\times$ 10 cm. The LCA is a modification of the CA. The two diverging metal walls of the horn antenna, which are parallel to the electric field, are replaced by lucite walls. Additionally, a PVC cone with a height of 5.5 cm is inserted in the applicator at the center of the aperture. Different

Fig. 1. Various applicators. (left) LA with the two diverging walls of the horn antenna parallel to the electric field made of lucite. (center) LCA similar to the LA with a PVC cone inserted in the center of the antenna. (right) CA made totally of metal.

TABLE I
ELECTRICAL PROPERTIES OF THE MATERIALS

MATERIAL	ϵ_r	σ (S/m)
De-ionized water	76.0	0.001
Lucite	2.59	0.003
PVC	2.2	0.004
Muscle phantom	57.0	1.2

cone angles have been tested, and it was found that the angle of 15° gave the best results. The LCA is described extensively in [4]. The various applicators are shown in Fig. 1.

B. Electromagnetic Modeling

The FDTD technique is used for modeling the LCA. The technique is well established in the field of biomedical applications of electromagnetic radiation [8], although most of the work performed with it in the area of hyperthermia concerns deep regional treatments.

The developed numerical model attempts to simulate the experimental setup as closely as possible. The assumed electrical properties of the materials are shown in Table I. The applicators are placed on top of a flat muscle-equivalent phantom constructed according to [9].

The size of the phantom used in the experimental measurements was $50 \times 50 \times 10$ cm^3. However, the simulated phantom dimensions were chosen to be $38 \times 30 \times 14$ cm^3, in order to reduce the computer memory requirements. The choice for these dimensions was based on the results presented in [6].

A uniform rectilinear mesh was used with a cell size of 0.2 cm. The total size of the computational domain (including the applicator) was $190 \times 150 \times 225$ cells. The domain was terminated with Mur's second-order absorbing boundary conditions [10], which are expected to be adequate in this case (see [11], [12]).

The metallic walls of the applicator were treated as perfect electric conductors (PECs) so that the "diagonal split cell model" [8] could be used in a straightforward manner for the diverging metallic walls of the applicator, which are oblique

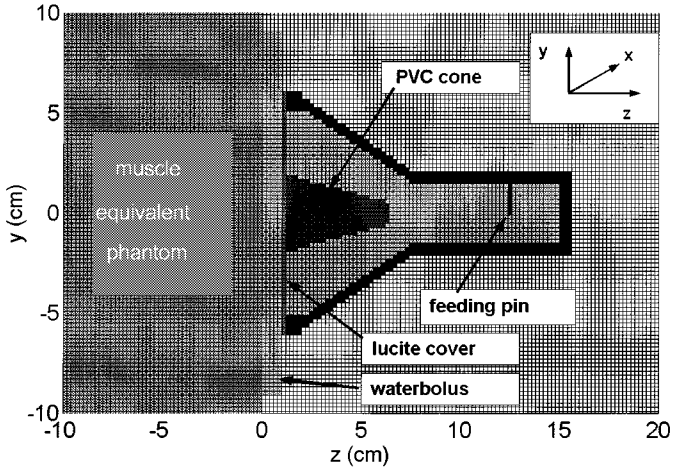

Fig. 2. Representation of the numerical model in two dimensions.

to the rectilinear mesh. This contour-path model is derived directly from Faraday's law and is simple to implement compared to the conformal modeling that had been used in other studies for horn antennas [13]. The simulations have shown that even this simple modification for the metallic walls gave better numerical results than the "staircasing" approach, which was, however, retained for the lucite walls and the PVC cone.

A sinusoidal signal at 433 MHz with a linear time ramp was used for the excitation. The total simulation time was 20 periods of the source signal. The CPU time for a simulation was about 10 h on a PC with an Intel Pentium II microprocessor at 450 MHz and 512-MB of RAM memory.

C. Thermographic SAR Measurements

The SAR distributions were measured experimentally with an infrared camera (AGA Thermovision System 680/102B, Lidingö, Sweden) interfaced to a PC. The applicators were placed on top of a semisolid muscle equivalent phantom ($50 \times 50 \times 10$ cm^3) [9]. Between the applicator and phantom, a waterbolus (a plastic bag filled with deionized water) was positioned. The measurement procedure is explained in detail in [4]. The measurements were performed according to the European Society for Hyperthermic Oncology (ESHO) quality assurance guidelines [3]. However, due to the low sensitivity of the camera, heating times of up to 1.5 min were used for the temperature to rise between 3 °C–6 °C in the phantom. Although this is slightly longer than the time specified in the ESHO guidelines, it is shown in [6] that it does not have an adverse effect in the resulting SAR distributions. The time that is necessary for the experimental assessment of a single SAR distribution in this manner is roughly 1 h. After each measurement, a period of 2–4 h is necessary for the phantom to reach again thermal equilibrium. Therefore, it is more convenient to acquire the 3-D SAR distribution in the phantom with a single computer simulation instead of several measurements.

III. RESULTS AND DISCUSSION

Numerical calculations have been performed for all three types of applicators of Fig. 1, i.e., the conventional applicator (CA), lucite applicator (LA), and LCA. However, results will be presented

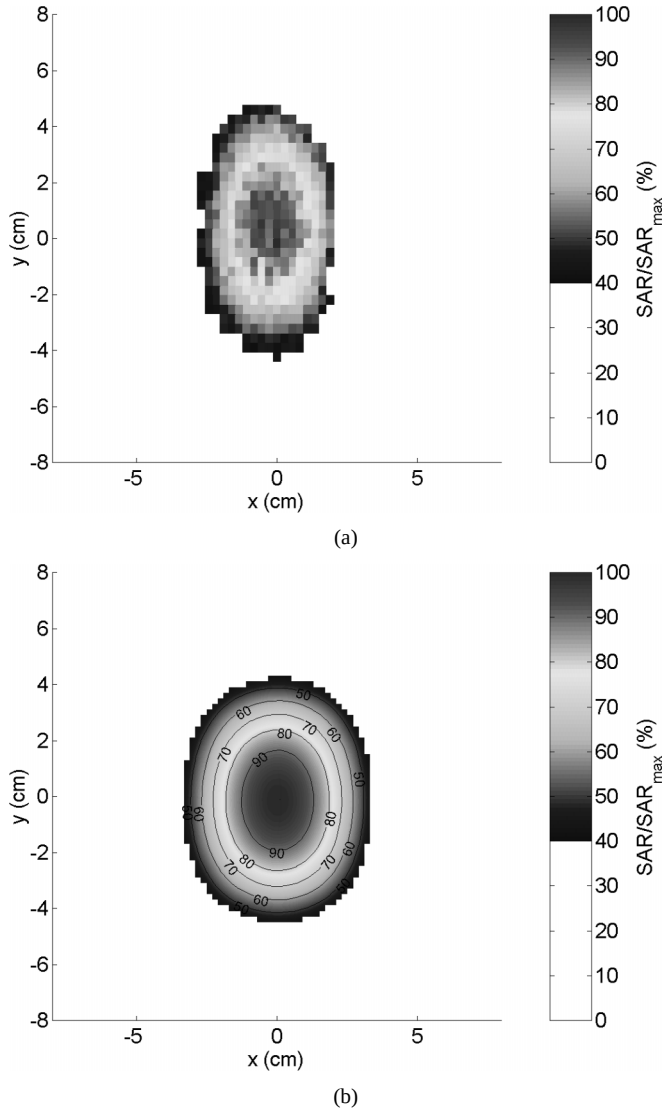

Fig. 3. SAR distributions (normalized to their maximum value) on the transverse cross section of a flat homogeneous muscle-equivalent phantom at a depth of 1 cm for a CA and a waterbolus of 1-cm thickness. (a) Measured distribution. (b) Predicted distribution.

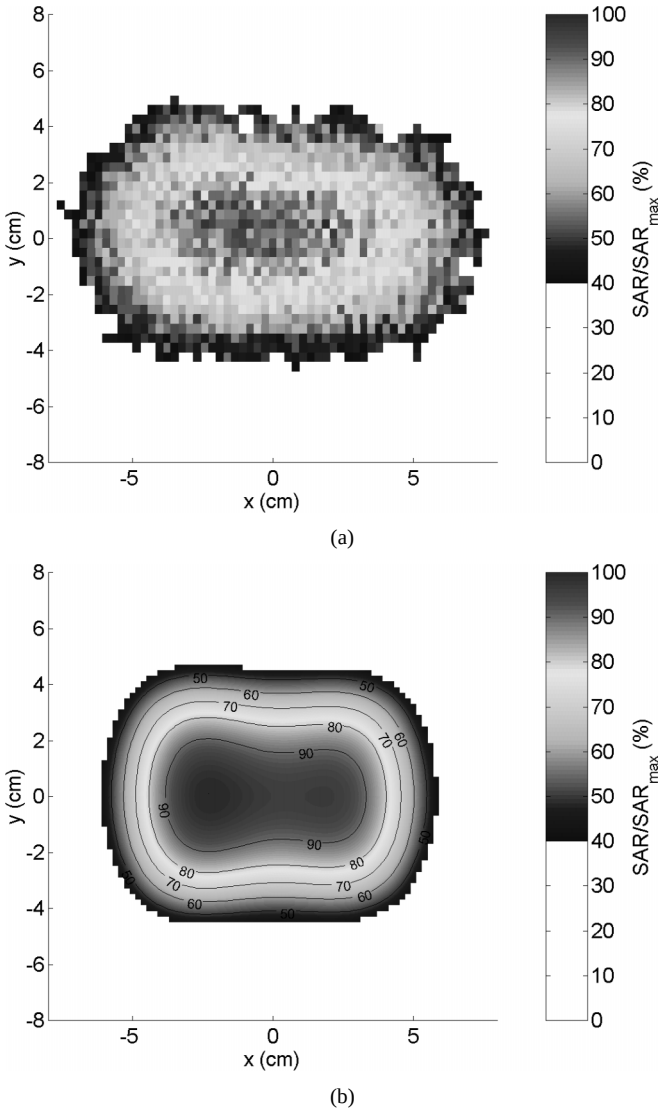

Fig. 4. SAR distributions (normalized to their maximum value) on the transverse cross section of a flat homogeneous muscle-equivalent phantom at a depth of 1 cm for an LCA and a waterbolus of 1-cm thickness. (a) Measured distribution. (b) Predicted distribution.

mainly for the conventional waveguide and LCA, which are the only ones to have been used in clinical practice. The discretized model that was used for the simulations is shown in Fig. 2. A finite-size waterbolus of $18 \times 18 \times 1$ cm^3 similar to the one used during measurements was included in the model.

On the cross section of the muscle-equivalent phantom normal to the propagation direction, the SAR distributions are compared at a depth of 1 cm. Figs. 3 and 4 show the predicted and measured distributions for the two types of applicators. The values are normalized to the maximum value of each distribution. For clarity, only ISO–SAR values above 40% are plotted. A comparison of the predicted and measured SAR profiles along the main axes of the applicator's aperture is presented in Figs. 5 and 6. The SAR distributions in these figures are normalized to the maximum along each axis. The normalization is performed in a way that the measured and predicted distributions have the same baseline.

It can be seen from Figs. 3–5 that there is a very good agreement between the predicted and measured distributions for both applicators. This was achieved by using a cell size of 0.2 cm in order to correctly model the lucite cover in front of the radiating aperture. Without this cover, for a coarse grid of 0.5 cm, the predicted results differed considerably from the measured distributions. This verifies the finding that the presence of thin dielectric layers in front of the applicator has an impact on the SAR distribution [14].

The difference between predicted and measured results is studied in Fig. 7, which shows the SAR relative difference (SRD) in absolute values between the measured and predicted normalized distributions for the CA and LCA. The differences are calculated for values within the EFS, i.e., $\mathrm{SAR} = 50\%$. The figure shows that, within the EFS, the mean deviation of the measured values from the predicted ones is about 14% for the CA and 12% for the LCA. It must be noted at this point that the resolution of the infrared camera is poor with a pixel size of roughly 4 mm $\times$ 3 mm. Furthermore, heat diffusion during measurements can alter significantly the measured distributions [15].

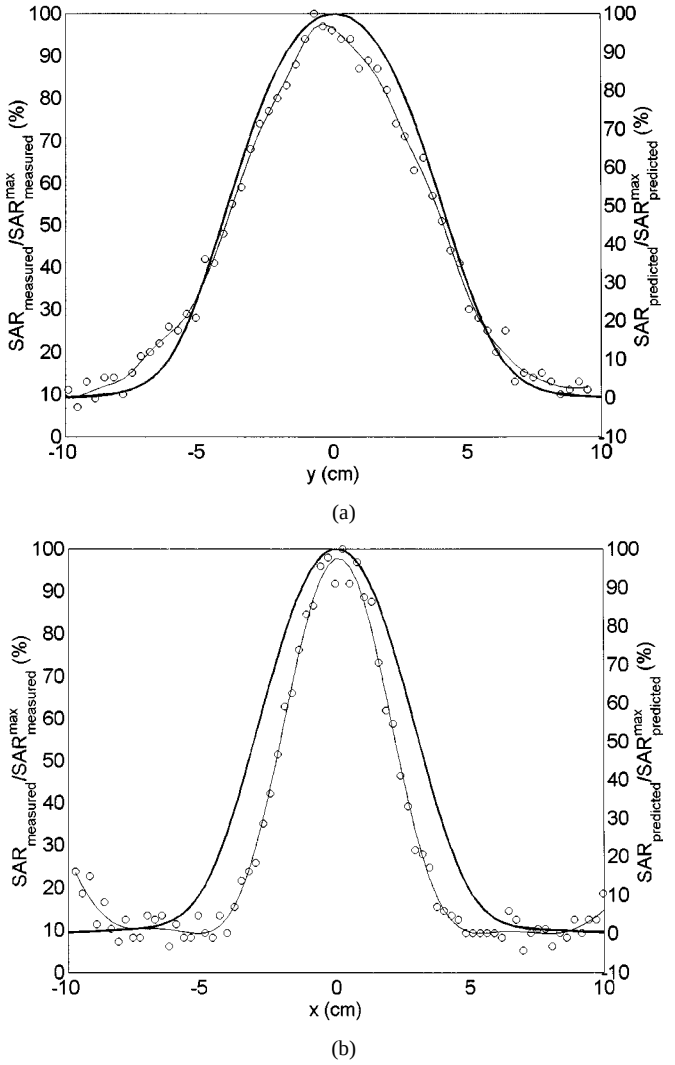

Fig. 5. SAR distribution along the aperture axis of the CA. Axis: (a) parallel and (b) perpendicular to the electric field. The predicted (thick line), measured (circle points), and spline fit for the measured (thin line) distributions are also given.

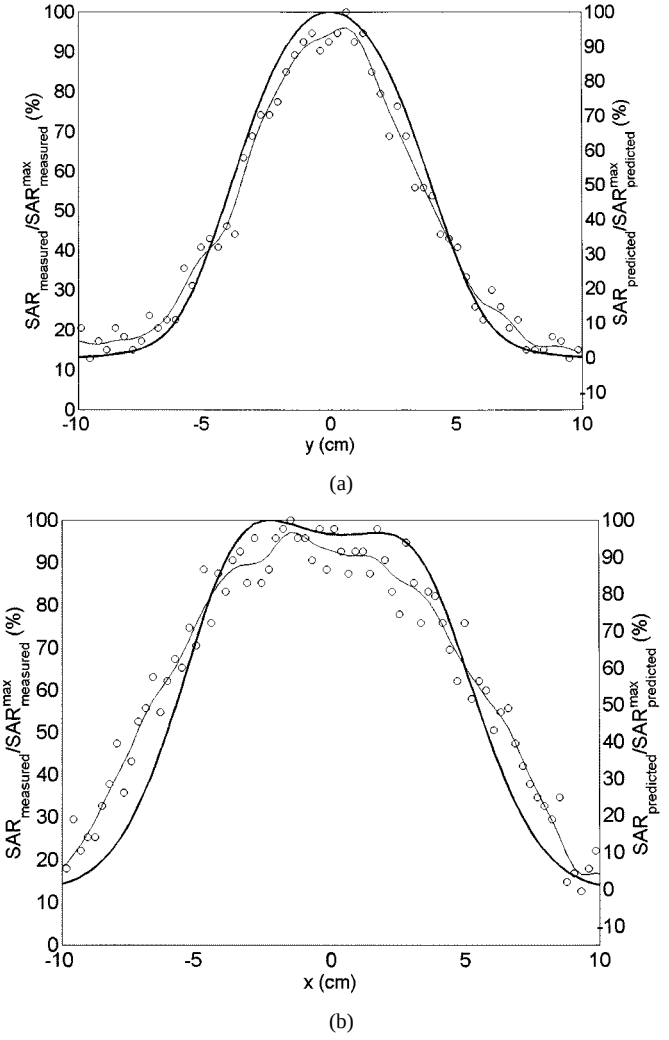

Fig. 6. SAR distribution along the aperture axis of the LCA. Axis: (a) parallel and (b) perpendicular to the electric field. The predicted (thick line), measured (circle points), and spline fit for the measured (thin line) distributions are given.

An important quantity for the characterization of superficial hyperthermia applicators is their EFS. Table II summarizes the results with respect to the EFS for all three applicator types. The predicted values are given at 0.8-, 1-, and 1.2-cm depth to show the steepness of the EFS decay.

The results verify that the LCA has an increased EFS compared to the other applicator types. This is achieved in the two steps that were considered for its development, as they are described in [4].

Along the direction of propagation, it was not possible to measure the SAR distribution. The calculated SAR distributions on the H- and E-field planes show that there is little difference among the three applicator types for the energy deposition patterns inside the phantom as a function of depth. Nevertheless, the LCA is still slightly superior to the other two applicator types in terms of the penetration depth. Its penetration depth—calculated with an exponential fit of the numerical results—was found to be 3.6 cm compared to 3.2 cm for the CA and 3.1 cm for the LA. The penetration depth for plane-wave exposure at this frequency is reported to be 3.56 cm [3], [9].

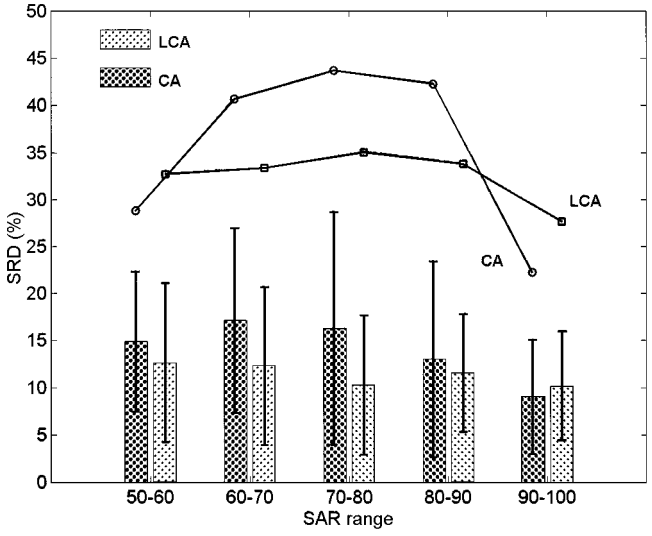

Fig. 7. SRD between the predicted and measured distributions for the CA and LCA. The SRD is calculated for SAR values that fall into the EFS of the applicators and for ranges of 10% SAR. The bars represent the mean value per range of values, the error bars represent the corresponding standard deviation, and the lines indicate the maximum difference for each SAR range.

TABLE II
MEASURED AND PREDICTED EFS FOR THE THREE APPLICATORS

APPLICATOR	MEASURED AT 1 cm	PREDICTED AT 0.8 cm	PREDICTED AT 1 cm	PREDICTED AT 1.2 cm
Conventional	32 cm^2	40.92 cm^2	40.16 cm^2	39.64 cm^2
Lucite	67 cm^2	54.64 cm^2	54.32 cm^2	54.08 cm^2
Lucite cone[a]	91 cm^2	85.92 cm^2	84.88 cm^2	83.40 cm^2

[a] The average measured value for six LCAs was 91 ± 6 cm^2 (one standard deviation).

TABLE III
CAPABILITY OF APPLICATORS TO DELIVER POWER TO THE PHANTOM

APPLICATOR	SAR_{max} (W/kg/W_{in}) at surface	SAR_{max} (W/kg/W_{in}) at 1 cm	ΔT (°C/min/W_{in}) at surface	ΔT (°C/min/W_{in}) at 1 cm
Conventional	5.25	2.93	0.0875	0.0488
Lucite	4.15	2.15	0.0692	0.0358
Lucite cone	2.81	1.55	0.0468	0.0258

The efficiency of the applicators has also been calculated from the ratio of the power absorbed in the muscle phantom to the power input to the applicator. It was found that the efficiency of all three applicators was about 48%. Table III contains information about the calculated maximum SAR, which is achieved at the surface of the muscle phantom and at 1-cm depth in it per watt of input power. It is assumed that the muscle-equivalent phantom has a density of $\rho = 1000$ kg/m^3 [16]. The maximum temperature rise per watt of input power for a heating period of 1 min can be estimated from the maximum SAR values,[3] assuming that the specific heat of the phantom is 3600 J/kg/°C [16].

IV. CONCLUSIONS

A 3-D model based on the FDTD method was developed for the study of superficial hyperthermia applicators. With this model, it is feasible to further investigate the three applicator types considered. The results have verified that the LCA has a better performance than the other two applicator types in terms of EFS and, moreover, they have shown that the penetration depth of the LCA is higher than for the other two applicators.

The approach described in this paper allows a direct 3-D analysis of the treatment setup. This will certainly facilitate the determination of clinically significant treatment factors and help improve treatment quality.

REFERENCES

[1] International Collaborative Hyperthermia Group, "Radiotherapy with or without hyperthermia in the treatment of superficial localized breast cancer—Results from five randomized controlled trials," *Int. J. Radiat. Oncol. Biol. Phys.*, vol. 35, pp. 731–744, 1996.

[2] M. D. Sherar, F. F. Liu, M. Pintilie, W. Levin, J. W. Hunt, R. Hill, J. W. Hand, C. C. Vernon, G. C. van Rhoon, J. van der Zee, D. G. González-González, J. D. P. van Dijk, J. Whaley, and D. Machin, "Relationship between thermal dose and outcome in thermoradiotherapy treatments for recurrences of breast cancer in a randomized phase III trial," *Int. J. Radiat. Oncol. Biol. Phys.*, vol. 39, pp. 371–380, 1997.

[3] J. W. Hand, J. J. W. Lagendijk, J. B. Andersen, and J. C. Bolomey, "Quality assurance guidelines for ESHO protocols," *Int. J. Hyperthermia*, vol. 5, pp. 421–428, 1989.

[4] G. C. van Rhoon, P. J. M. Rietveld, and J. van der Zee, "A 433 MHz lucite cone waveguide applicator for superficial hyperthermia," *Int. J. Hyperthermia*, vol. 14, pp. 13–27, 1998.

[5] P. J. M. Rietveld, W. L. J. van Putten, J. van der Zee, and G. C. van Rhoon, "Comparison of the clinical effectiveness of the 433 MHz lucite cone applicator with that of a conventional waveguide applicator in applications of superficial hyperthermia," *Int. J. Radiat. Oncol. Biol. Phys.*, vol. 43, pp. 681–687, 1999.

[6] P. J. M. Rietveld, M. L. D. Lumori, J. W. Hand, M. V. Prior, J. van der Zee, and G. C. van Rhoon, "Effectiveness of the Gaussian beam model in predicting SAR distributions from the lucite cone applicator," *Int. J. Hyperthermia*, vol. 14, pp. 293–308, 1998.

[7] P. J. M. Rietveld, M. L. D. Lumori, J. van der Zee, and G. C. van Rhoon, "Quantitative evaluation of 2×2 arrays of lucite cone applicators in flat layered phantoms using Gaussian-beam-predicted and thermographically measured SAR distributions," *Phys. Med. Biol.*, vol. 43, pp. 2207–2220, 1998.

[8] A. Taflove, *Computational Electrodynamics: The Finite-Difference Time-Domain Method*. Norwood, MA: Artech House, 1995.

[9] A. W. Guy, "Analysis of electromagnetic fields induced in biological tissues by thermographic studies on equivalent phantom models," *IEEE Trans. Microwave Theory Tech.*, vol. MTT-19, pp. 205–214, Feb. 1971.

[10] G. Mur, "Absorbing boundary conditions for the finite-difference approximation of the time-domain electromagnetic field equations," *IEEE Trans. Electromag. Compat.*, vol. EC-23, pp. 377–382, Apr. 1981.

[11] P.-Y. Cresson, C. Michel, L. Dubois, M. Chive, and J. Pribetich, "Complete three-dimensional modeling of new microstrip-microslot applicators for microwave hyperthermia using the FDTD method," *IEEE Trans. Microwave Theory Tech.*, vol. 42, pp. 2657–2666, Dec. 1994.

[12] L.-K. Wu and W. K. Nieh, "FDTD analysis of the radiometric temperature measurement of a bilayered biological tissue using a body-contacting waveguide probe," *IEEE Trans. Microwave Theory Tech.*, vol. 43, pp. 1576–1583, July 1995.

[13] D. S. Katz, M. J. Piket-May, A. Taflove, and K. R. Umashankar, "FD-TD analysis of electromagnetic wave radiation from systems containing horn antennas," *IEEE Trans. Antennas Propagat.*, vol. 39, pp. 1203–1212, Aug. 1991.

[14] F. Rossetto, P. R. Stauffer, V. Manfrini, C. J. Diederich, and G. B. Gentili, "Effect of practical layered dielectric loads on SAR patterns from dual concentric conductor microstrip antennas," *Int. J. Hyperthermia*, vol. 14, pp. 553–571, 1998.

[15] E. G. Moros and W. F. Pickard, "On the assumption of negligible heat diffusion during the thermal measurement of a nonuniform specific absorption rate," *Radiat. Res.*, vol. 152, pp. 312–320, 1999.

[16] J. B. Leonard, K. R. Foster, and T. W. Athey, "Thermal properties of tissue equivalent phantom materials," *IEEE Trans. Biomed. Eng.*, vol. BME-31, pp. 533–536, July 1984.

[3] Using the equation $\Delta T = (\mathrm{SAR} \cdot \Delta t / c)$, where Δt is the heating time and c is the specific heat.

T. Samaras (S'93–A'97), photograph and biography not available at time of publication.

P. J. M. Rietveld, photograph and biography not available at time of publication.

G. C. van Rhoon (M'98), photograph and biography not available at time of publication.